A collaboration to design and prepare multifunctional carbon nano-onion-based materials for energy storage and conversion, between Dr. Plonska-Brzezinska at the University of Bialystok and the Carbon Nanomaterials Group of Prof. Echegoyen at the University of Texas.

Title: Carbon nano-onions for supercapacitor electrodes: recent developments and applications

This critical review covers the use of carbon nano-onion (CNO) based materials for electrochemical capacitor (EC) electrodes. The advantages of exohedrally functionalized CNOs, the challenges and applications, especially in EC electrodes, are discussed in detail through an extensive analysis of the literature.
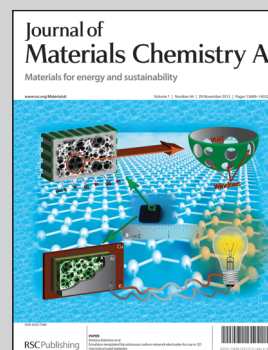
Carbon nano-onions for supercapacitor electrodes: recent developments and applications

Marta E. Plonska-Brzezinska*[a] and Luis Echegoyen*[b]

This critical review covers the use of carbon nano-onion (CNO) based materials for electrochemical capacitor (EC) electrodes. The performance of CNO capacitors is reviewed in detail and compared to the results obtained using different carbon nanostructures. The physico-chemical *vs.* electrochemical properties of CNOs are discussed. Their advantages, challenges and applications, especially in EC electrodes, are discussed in detail through an extensive analysis of the literature. Exohedral carbon nano-onions are much less limited by mass transfer kinetics; they show low resistance and can operate over a wide voltage and temperature window, at very high charge–discharge rates with almost unlimited cyclabilities. Although carbon nano-onions make excellent supercapacitor electrode materials, many challenges still remain, particularly to characterize and understand the physical, chemical, and electrochemical interactions within multicomponent systems that contain CNOs. The full potential of carbon nano-onions as electrochemical power sources has not been realized yet, but as outlined in this review, the future looks very promising.

[a]Institute of Chemistry, University of Bialystok, Hurtowa 1, 15-399 Bialystok, Poland. E-mail: mplonska@uwb.edu.pl; Fax: +48 85 747 0113; Tel: +48 85 745 7816

[b]Department of Chemistry, University of Texas at El Paso, 500 W. University Ave., El Paso, TX 79968, USA. E-mail: echegoyen@utep.edu; Fax: +1 915 7478807; Tel: +1 915 7477573

1. Introduction

Currently, some of the most effective and practical technologies for electrochemical energy conversion and storage include fuel cells, batteries, capacitors and electrochemical capacitors (ECs), whose relative performance properties are shown in Fig. 1.[1,2] Major advances in designing and developing new EC materials are difficult because of the required energy densities and the typically high production costs. One obvious approach is to

Marta E. Plonska-Brzezinska received her PhD in Chemistry at the University of Bialystok (2005) working with Prof. Krzysztof Winkler. After a Doctoral Research Fellowship at the University of California, Davis, working with Prof. Alan Balch and a Postdoctoral Fellowship at the University of Clemson, working with Prof. Luis Echegoyen, she came back to her Alma Mater. Her research focuses principally on electrochemical properties of fullerenes and carbon-based materials, and designing and creating multifunctional nanoarchitectures for energy storage and conversion. She is an Assistant Professor of Chemistry at the University of Bialystok, and a recipient of an NCN SONATA BIS Starting Grant.

Prof. Luis Echegoyen obtained both a BSc and a PhD in Physical Chemistry from the University of Puerto Rico in Rio Piedras (1971 and 1974, respectively). After a three year industrial position at Union Carbide and several professorships at the Universities of Puerto Rico, Maryland, and Miami, in 2002 he was appointed as the Chair of the Department of Chemistry at Clemson University. Later he served as Division Director for Chemistry at the National Science Foundation for 4 years (2006–2010), and more recently, he became the Robert A. Welch Professor of Chemistry at the University of Texas, El Paso in 2010. His research interests include fullerene chemistry, electrochemistry, and supramolecular chemistry, with special emphasis on endohedral fullerenes and photovoltaics.
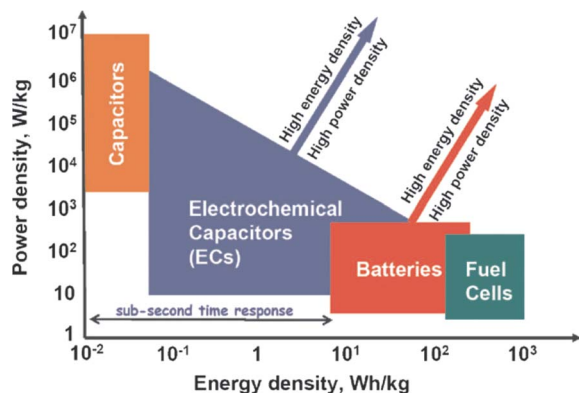
This journal is © The Royal Society of Chemistry 2013

J. Mater. Chem. A, 2013, **1**, 13703–13714 | **13703**

Fig. 1 Comparison of the operational characteristics of energy storage and conversion devices, with arrows indicating the goal of improving both energy and power density for batteries and electrochemical capacitors (reproduced with permission from Elsevier).[2]
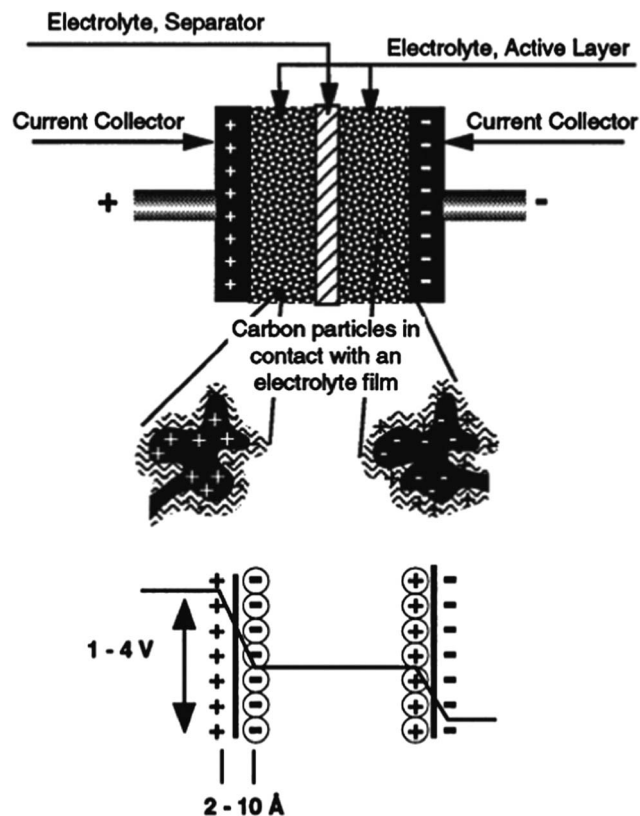

Fig. 2 Schematic representation of a double-layer capacitor and illustration of the potential drop at the electrode–electrolyte interface (reproduced with permission from Elsevier).[5]

develop new materials with improved properties for EC electrodes. The discovery of nanostructured forms of carbon has had a dramatic impact on the design and preparation of new electrode materials. The unique combination of very favorable mechanical properties of these carbon nanostructures with similarly convenient chemical and physical properties, namely relatively high surface-to-volume ratio, reasonably high conductivity, high thermal stability, excellent corrosion resistance, controlled size distribution, satisfactory compatibility in composite materials and cost effectiveness, make these very attractive as supercapacitor materials.[3,4]

Carbon nanostructures comprise a wide number of nanoforms with different sizes, shapes and hybridization states, such as porous activated, templated and carbide derived carbon. These structural variations play a significant role in the properties and specific applications. Carbon materials are widely used in ECs because of their low cost and morphological versatility existing as powders, fibers, felts, composites, mats, and foils. Efficient charging of electrical double capacitor layers requires materials with high surface areas and pores that are appropriate to accommodate different sized ions, which is crucial for supercapacitor performance.[5] Carbon electrode polarizabilities and electrical conductivities strongly depend on their physico-chemical properties, such as hybridization, microtexture and heteroatom content.[4] Among the most studied nanocarbon forms that are getting close to finding practical applications in EC devices are the carbon nanotubes (CNTs), carbon nano-onions (CNOs), and graphene. In the current review, we focus on the electrochemical performance of carbon nano-onions and their composites for potential use as supercapacitor electrodes.

2. Principle of a supercapacitor

An electrochemical capacitor, also called a supercapacitor or ultracapacitor, is a device able to accumulate charges at the electrode–electrolyte interface, as shown in Fig. 2.[5] The most important part of an EC is the electrode composition, typically

fabricated from nanostructured materials with high surface areas and high porosities.[2–8] Theoretically, the higher the surface areas and the electrolyte concentrations, the higher the capacitance values. The charges are stored and separated at the interface between the electrode surface and the electrolyte. This electrical interface can be described as a capacitor with an electrical double-layer capacitance using the following equation (eqn (1)):[5,7]

$$C = \left(\frac{\varepsilon_{\mathrm{r}}\varepsilon_{\mathrm{o}}}{d}\right)A \tag{1}$$

where, ε_{r} is the relative permittivity and is a dimensionless constant, ε_{o} is the permittivity of vacuum, A is the specific surface area of the electrode, and d is the effective thickness of the electrical double layer.

The total capacitance of ECs built from electrode materials with significantly different surfaces is controlled by the electrode exhibiting the smaller value between the anode capacitance C_{a} and the cathode capacitance C_{c}, according to eqn (2):[8]

$$\frac{1}{C} = \frac{1}{C_{\mathrm{a}}} + \frac{1}{C_{\mathrm{c}}} \tag{2}$$

An increase of the capacitor voltage (U) causes a significant enhancement of the power (P) and energy (E) according to eqn (3) and (4):[6,7,9]

$$E = \frac{1}{2}CU^2 \tag{3}$$

13704 | *J. Mater. Chem. A*, 2013, **1**, 13703–13714

This journal is © The Royal Society of Chemistry 2013

Table 1 Different carbon structures used in EDLCs[6,9–16]

Material	Carbon nano-onion	Carbon nanotube		Graphene	Activated carbon	Carbide derived carbon	Templated carbon
		SWNT	MWNT				
Conductivity	High	High	High	High	Low	Moderate	Low
Volumetric capacitance (g cm^{-3})	Low	Low 0.3	Low	Moderate	High	High	Low
Specific capacitance (F g^{-1})	30	50–70^a	15–100	<100^d; <260	<200^a	100–130^g	100–350
Specific surface area (BET) (m^2 g^{-1})	380–600	1000	100–410^b	<1500; 2670^c	<3000^f	1000–3000^e	500–3000
Cost	High	High	High	Moderate	Low	Moderate	High

^{a} Organic electrolytes from ref. 25. ^{b} From ref. 6. ^{c} Theoretical value. ^{d} Nonaqueous electrolytes from ref. 26. ^{e} From ref. 27. ^{f} From ref. 28. ^{g} From ref. 29.

$$P = \frac{U^2}{4R_S} \qquad (4)$$

where R_S stands for the equivalent series resistance. To achieve a supercapacitor with high performance, a high cell voltage and low R_S are required.

The improved performance of supercapacitors requires the selection of appropriate electrode materials. As already discussed, the electrode material should possess a large conductive surface area with reasonably high electrochemical cycling stability, fast charge–discharge processes, reasonably low self-discharging, high thermal stability and well defined pore size distributions.[4,7,8]

The charge on the electrode surface–electrolyte interface can be stored *via* electrostatic interactions (electrical double layer capacitors, EDLCs) or by faradaic processes (pseudocapacitors, also called faradaic supercapacitors, FSs).

EDLCs store the energy by ion adsorption and the capacitance is associated with an electrode-potential-dependent accumulation of charge at the electrode interface through polarization. During the charging–discharging process of carbon-based EDLCs, the electrode material is not electrochemically active.[2–8]

The electrode materials in FSs are electrochemically active and fast faradaic reactions are involved, requiring charge transfer across the double layer. Pseudocapacitance arises when the charge (Δq) required for an electrode process requires a change of potential (ΔU), and corresponds to the derivative ($d\Delta q/d\Delta U$).[10]

The difference in charge accumulation in processes in EDLCs and FSs leads to the different magnitudes of their capacitances. Since electrode polarization in FSs is associated with the conversion of chemical into electrical energy, the magnitude of the pseudocapacitance is higher when compared to that for EDLCs. FSs have relatively poor electrochemical cycling stability, low power densities and high resistances. Pseudocapacitances strongly depend on the chemical affinity of carbon materials for the ions adsorbed on the electrode surface. In most of the cases, double layer capacitance and pseudocapacitance co-exist. For instance, about 1–5% of the total capacitance of an EDLC derives from the presence of pseudocapacitance contributions, typically due to the presence of surface oxygen-functionalities.[4] On the other hand, FCs always exhibit some electrostatic double-layer capacitance, which is proportional to their electrochemically accessible interfacial areas (about 5–10%).[4]

The reason for using carbon-based materials in ECs is due to the unique combination of their chemical and physical properties. Carbon-based EDLCs constitute more than 80% of the commercially manufactured ECs.[11] Carbon-based electrodes are easily polarized and their conductivities strongly depend on their physico-chemical properties. The double-layer capacitance is associated with the electrode–electrolyte interface, which is a function of the type of carbon used and its preparation protocol (see Table 1). In this review, we discuss the physico-chemical as well as the electrochemical properties of the CNO-based materials and their competitive advantages relative to other carbon-based materials.
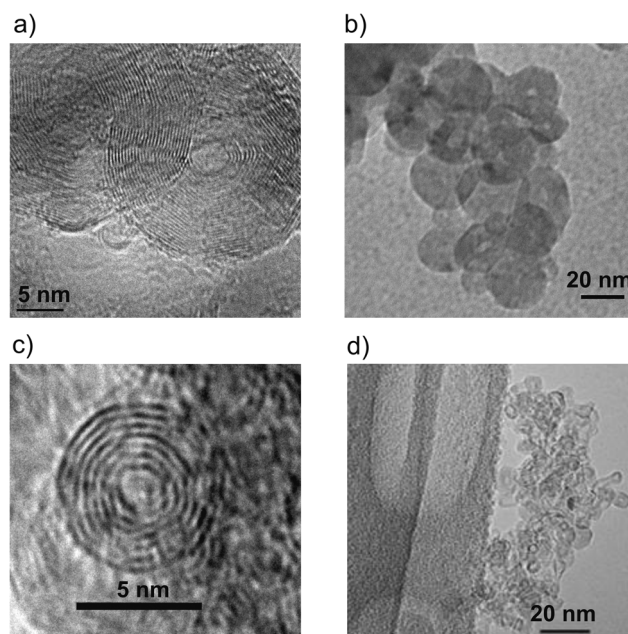

Fig. 3 (a) High- and (b) low-resolution TEM images of CNOs from arcing graphite under water (A-CNOs). (c) High- and (d) low-resolution TEM images of CNOs from thermally annealing nanodiamonds (N-CNOs). TEM was performed with lacey-carbon grids. Scale bars represent 20 nm and 5 nm in the low- and high-resolution images, respectively (reproduced with permission from Wiley).[30]

This journal is © The Royal Society of Chemistry 2013

J. Mater. Chem. A, 2013, **1**, 13703–13714 | **13705**

3. Physico-chemical *vs.* electrochemical properties of CNOs

Among the less studied carbon nanostructures are those that are difficult to obtain in high yields, such as carbon nanohorns, nanocups and peapods. Carbon nano-onions (CNOs) were discovered in 1992 by Ugarte,[12] and until quite recently they were seldom studied, mainly because of their unavailability and lack of convenient methods for their preparation and separation.

Carbon nano-onions are spherical and typically 4–25 nm particles, consisting of concentric shells of graphitic carbon, that can also be described as multi-shelled fullerenes (Fig. 3).[17] Different methods have been used for CNO synthesis, mainly vacuum annealing of nanodiamonds (NDs),[13] graphite arc discharge underwater,[14] flash pyrolysis,[15] ion implantation into copper and silver,[16] vapor deposition,[17] stainless steel autoclave reactions,[18] and laser irradiation.[19] Most of these methods lead to low yields and/or many byproducts. For applications such as EC electrodes, large quantities of material are required. The preparation method controls the final physico-chemical properties, including their size (see Fig. 3a and c). It has already been reported that CNOs produced by arcing graphitic rods under water or by annealing of 5 nm nanodiamond particles exhibit very different physical properties and chemical reactivities.[17] Given the easier functionalization and higher thermal stability of the CNOs prepared from NDs, they are the most obvious choice for studying the potential applications of these multi-shelled fullerene structures.

CNOs were obtained by annealing nanodiamonds with a crystal size between 4 and 6 nm. NDs were placed in a graphite crucible and transferred to an Astro carbonization furnace. Annealing of ultradispersed nanodiamonds was performed at 1650 °C under a 1.1 MPa He atmosphere with a heating ramp of 20 °C min^{-1}. The final temperature was maintained for one hour, and then the material was slowly cooled to room temperature over a period of one hour. The furnace was opened, and the transformed CNOs were annealed in air at 400 °C to remove any amorphous carbon. Carbon nano-onions formed from NDs by vacuum annealing can be also prepared at different temperatures. CNOs obtained in the 1200–2000 °C temperature range exhibit structures with different degrees of graphitization and microtexture.[20] High-resolution transmission electron microscopy (HRTEM) analysis demonstrated that NDs are transformed into spherical CNOs by annealing at 1700 °C, and finally into polyhedral onions above 1900 °C.[21] Intershell spacings between graphitic shells in CNOs estimated from TEM diffraction patterns are typically around 0.335 nm, similar to the interlayer distance in highly oriented pyrolytic graphite (HOPG).[22] One of their most remarkable properties is self-compression when exposed to electron or ion irradiation at high temperature.[23] The distance between the compressed graphitic shells can reach values as low as 0.22 nm.[24]

Using electron spin resonance (ESR) spectroscopy it was found that spherical onions show only a narrow ESR signal with a *g* value of 2.0020, arising from the dangling bonds associated with structural defects in the onions.[30] HRTEM, Raman and electron-energy-loss spectroscopy (EELS) studies suggest the presence of π electrons.[31] The EELS studies of concentric-shell fullerenes with a narrow diameter distribution showed no change in the electronic properties of CNOs as a function of the diameter between 4 and 8 nm.[30] From electron diffraction studies it was found that there are many similarities to strongly disordered polycrystalline graphite. In contrast to single-shell fullerenes, a finite dispersion of the π and the π1s plasmons, which is about two-thirds of that in graphite, was observed. These results also suggest that spherical onions consist of small domains of graphitic sp^2 sheets with dangling bond defects in the periphery. π electrons in spherical CNOs are thus localized in the small domains and do not act as conduction electrons. On the other hand, an additional broad signal due to conduction π electrons appears for polyhedral onions, suggesting that further graphitization increases and leads to delocalization of π electrons. These results strongly suggest that the structure of spherical carbon nano-onions is far from perfectly closed graphitic shells; they likely contain multiple defects such as dangling bonds. Thus CNOs can be conceptualized as intermediate entities between fullerenes and graphite, and can be defined as spherical graphitic nanostructures.

A good correlation has also been found between the value of the capacitance and the microtextural characteristics of CNO particles between 5 and 15 nm in size.[33] However, less attention has been paid to the capacitance behaviour of CNO electrodes, which exhibit rather unique parallel differential capacitance–potential curves rather than the common bell- or concave-shaped curves.[34] This property greatly favors the stable performance of supercapacitors, which is characteristic of ideal double layer capacitance and of fast kinetic processes occurring at the carbon–electrolyte interface (see Fig. 4a–c).[33,35] The sign of the current is immediately switched upon reversal of the potential.[33] Energy storage is purely electrostatic and the current is independent of the applied potential.[33] The symmetry of the CVs gives insights into the ion size/pore size relationship as well as the carbon–electrolyte interactions.

A direct correlation between the symmetry of the CVs and the preparation temperature of the carbon nanostructures was found (see Fig. 4a–d).[33] The electrochemical properties of the best performing carbon nano-onion samples, prepared at 1800 °C, were compared to those of activated carbon (AC), carbon black (CB) and NDs, as a function of the sweep rates (see Fig. 4e and f). At the slower scan rates, AC exhibited the highest capacitance, but at 15 V s^{-1} CNOs (1800 °C) showed capacitive behaviour as high as CB. CNOs (1800 °C) exhibit the largest energy storage capacity at faster scan rates (see Fig. 4f): the power density normalized to the estimated volume of the cavities was 195.0 W cm^{-3} (132.9 W cm^{-3} for AC) and the energy density was 2.9 mW h cm^{-3} (2 mW h cm^{-3} for AC).[33]

The capacitance depends on the specific surface area of the electrode material. Nitrogen adsorption/desorption isotherms also provide information about the capacitive performance. The specific surface area (BET, surface area determined by the Brunauer, Emmett, and Teller method)[36] for CNOs ranges from about 380 to 520 m^2 g^{-1} depending on the preparation temperature (see Table 2).[32] The specific surface area of CNOs is

13706 | *J. Mater. Chem. A*, 2013, **1**, 13703–13714

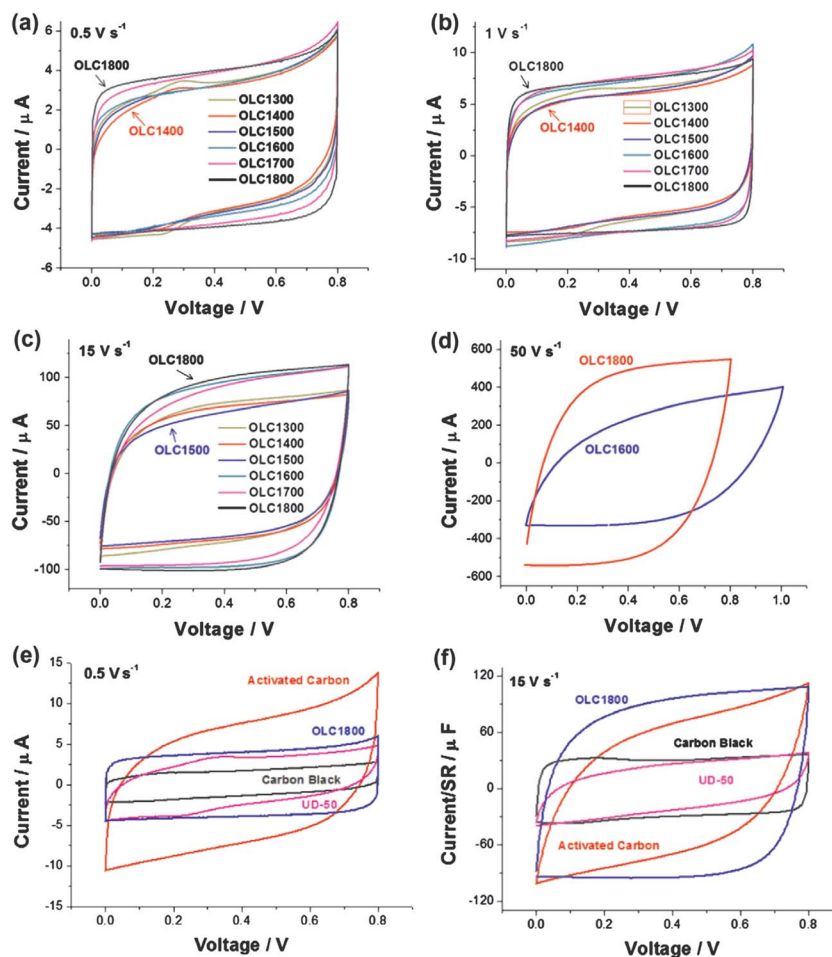This journal is © The Royal Society of Chemistry 2013

Fig. 4 Cyclic voltammetry of NDs, CNOs, CB and AC in 1 M H_2SO_4 at different scan rates. Comparison of CNOs at different scan rates at (a) 0.5, (b) 1, (c) 15 and (d) 50 V s^{-1}. CNOs (1800 °C) and other carbon materials at (e) 0.5 and (f) 15 V s^{-1}. The current is normalized by the scan rates (SRs) to obtain the capacitance (μF) (reproduced with permission from Elsevier).[33]

Table 2 Specific surface area variation of NDs annealed at different temperatures[32]

	Annealing temperature (°C)				
	ND	1200	1500	1800	2000
Average pore size (nm)	5	6	6	6	5
Specific surface area (BET) (m² g⁻¹)	380	500	510	520	460

lower than for many carbon materials, such as SWNTs, graphene, activated carbon, and carbide derived or templated carbon, but it is fully accessible for ion adsorption. Therefore they exhibit high electrical conductivities that result in high power with a limited capacitance of 30 F g^{-1} for non-modified CNOs (see Table 1).[34] This comparison shows that CNOs possess better mesoporous characteristics than many carbon-based materials.

Although generally higher surface area leads to higher capacitance, the relationship between these two is typically more complicated. Since the specific surface area and the electrochemically accessible area are not necessarily equivalent, properties such as structure, porosity and layer thickness need to be determined. Li *et al.* suggested that the capacitance is strongly related to the mesopore (∼2 nm) surface area, rather than to the total BET surface area.[37,38] It has been repeatedly emphasized that a correlation between the pore size and the EDLC capacitance exists.[39] Carbon EDLC electrodes contain varying porosities that range from nanopores to larger nanometer and micron-sized pores created by the packing of the carbon particles on the electrode surface.[40] The definition of porosity includes both pore sizes and pore-size distribution over all specific surface areas (m² g⁻¹).[41] According to Largeot *et al.* the optimal pore size of the electrode material should be very close to the desolvated (bare) ion size, for both electrolytic solutions and for solvent-free room-temperature ionic liquids.[42] If the pore size is matched with the electrolyte ion size, high energy densities can be obtained.[31,33,34]

The pore size of carbon materials can be controlled depending on the precursor and the activation method, physical or chemical. Activation parameters, such as a temperature, time, and activating agent, affect the microporosity.[43,44]

Table 3 Electrical conductivity; measured at room temperature of the as-received ND and ND annealed at 1200 °C and 1800 °C[32]

Conductivity (S m^{-1})	ND	1200 °C	1800 °C
Powder	0.025	2.9	4
Electrode	0.02	0.33–0.5	2.5–3

Matching the pore/ion size is especially important for ionic liquids, which can provide a high energy density. Kondrat *et al.* combined theory and experiments to define the concept of "the best pore size" in terms of operating voltage and pore size dispersion. The main findings can be briefly summarized as follows:[45] (i) the energy density is a function of the pore width; (ii) the optimal pore size depends on the ion size and the operating voltage (larger voltages favor larger pore sizes for optimum energy density); and (iii) narrowing the pore size distribution leads to an increase in the stored energy density.[46] This means that *a monodisperse porous electrode, with a carefully selected pore size, would be ideal for the energy storage of nanoporous supercapacitors*.

Galvanostatic cycling measurements and electrochemical impedance spectroscopy provide information about capacitance changes with current density and the electrochemical frequency behaviour of the system, respectively.[32] Charge–discharge measurements revealed a dependence of the specific capacitance of CNOs with the degree of graphitization and the number of defects on the particle surfaces. Table 3 shows the variation of the electrical conductivity as a function of the annealing temperature of NDs.[32] After vacuum annealing of NDs, the resulting CNOs exhibit a mostly closed graphitic surface with a few defects which has been shown to be crucial for fast charging and discharging processes.

Gogotsi *et al.* combined theory and experiments to probe the dependence of CNO conductivity with the annealing temperature of NDs.[31,33,34,41] The main findings can be briefly summarized as follows: (i) CNOs produced at high temperatures behave as ideal supercapacitors;[47] (ii) electrode conductivity increases with the degree of surface graphitization, which is associated with decreased defect densities; (iii) the high-temperature annealed CNOs exhibit excellent electrical properties at any current, similar to MWNTs; (iv) at high frequencies, the behavior of CNO supercapacitors is mainly resistive and leads to high specific powers for up to 60 kW kg^{-1} of active material (for MWNTs it is 63 kW kg^{-1}); and (v) the normalized capacitance is comparable to that of mesoporous activated carbons.[48]

Recently, many efforts have been devoted to understanding the connection between the synthetic method and the physicochemical properties of CNOs.

4. Advantages and applications of CNOs

4.1. Advantages

Electrolyte. The electrolyte solution is usually the limiting component of the overall stability of electrochemical systems. The choice of electrolyte determines the series resistance of the capacitor.[7,8] According to Tanahashi *et al.*,[49] organic electrolytes can operate at high voltages (up to 3 V), which is desirable for high energy and power densities, while aqueous electrolytes exhibit higher capacitances. Carbon nanostructures like CNOs or CNTs provide easy access for ions at the carbon–electrolyte interface, and are defined as exohedral supercapacitors due to curvature effects.[50] Since exohedral carbons are much less limited by mass transfer kinetics, they show lower resistances and improved performances. Carbon nanoparticles, such as CNOs and CNTs, can provide high power due to fast ion sorption/desorption on their outer surfaces. Although graphene has recently attracted considerable attention in this context, it has not shown higher volumetric capacitances than other porous carbon forms.[12,51]

A nonporous CNO electrode contains nearly spherical particles with a concentric shell structure and narrow particle size distribution.[52] The closed structures of high temperature annealed CNOs enable their use in organic electrolytes at temperatures as low as −40 °C and in ionic liquid electrolytes at −50 °C.[53] CNO-based EDLCs can operate between −50 and 100 °C, over a wide voltage window (up to 3.7 V) and at very high charge–discharge rates, up to 20 V s^{-1}.[41] Pure room-temperature ionic liquids (RTILs) and their binary mixtures were studied as electrolytes near onion-like particles as a function of temperature.[39] At constant temperature the capacitance increases as the size/radius of the CNOs decreases. The effective thickness of CNO-based EDLCs was found to increase with decreasing temperature, demonstrating the positive temperature dependence (capacitance increases as temperature increases),[54] a trend also observed in high-temperature molten salts.[55]

High power density. Charge storage occurs at the surface of carbon-based electrodes. Since an EC stores charges both at the electrode surface and in the bulk near the surface of the solid electrode, the charge–discharge process is not limited by ionic conduction in the bulk solution. EC carbon-active materials display low energy densities (1–10 W h kg^{-1}) when compared with Li-ion cells (typically 150 W h kg^{-1}).[56] However, ECs can be fully charged and discharged in a short time (∼30 s).

The cavity microelectrode (CME) technique was used to screen the electrochemical properties of CNOs in EDLCs.[55,56] Pech *et al.* reported microsupercapacitors with powers per unit volume that are comparable to electrolytic capacitors, produced by electrophoretic deposition of a several-micrometre-thick layer of nanostructured carbon nano-onions.[57] With CNOs, a maximum power density was obtained that is 100 times higher than that with ACs, at close to 1 kW cm^{-3}. Current responses at different scan rates for CNOs prepared at different temperatures showed a linear relationship up to 3 V, indicating the high power and high rate capabilities (Fig. 5). CVs were recorded at scan rates from 1 to 200 V s^{-1}, and the system showed reproducible and stable capacitive behaviour for up to 10 000 cycles, and with a linear dependence of the discharge current on the scan rate and a low resistive contribution up to 100 V s^{-1} (Fig. 5b). However, as is shown in Fig. 6, the microdevices with AC showed higher capacitance (9 F g^{-1}) compared to CNOs (1.3 F g^{-1}), and the capacitance of the microdevices with AC fell quickly at higher scan rates, because of the limitation of ion transfer to the inner pores of AC.[56] Due to the better accessibility
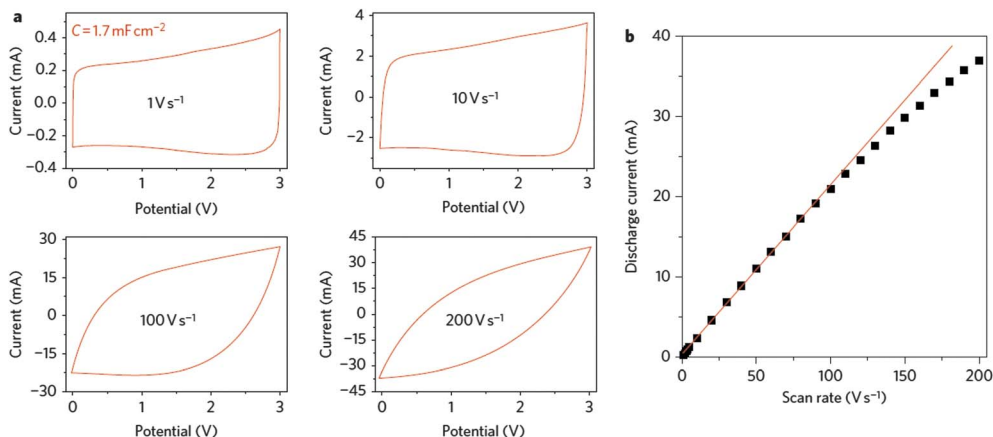
13708 | *J. Mater. Chem. A*, 2013, **1**, 13703–13714

This journal is © The Royal Society of Chemistry 2013

Fig. 5 Electrochemical characterization of microdevices: (a) CVs obtained at different scan rates in 1 M Et_4NBF_4/anhydrous propylene carbonate for electrochemical microdevices with a 7 μm thick CNO deposit; (b) evolution of discharge current *versus* scan rate (reproduced with permission from MPL).[57]
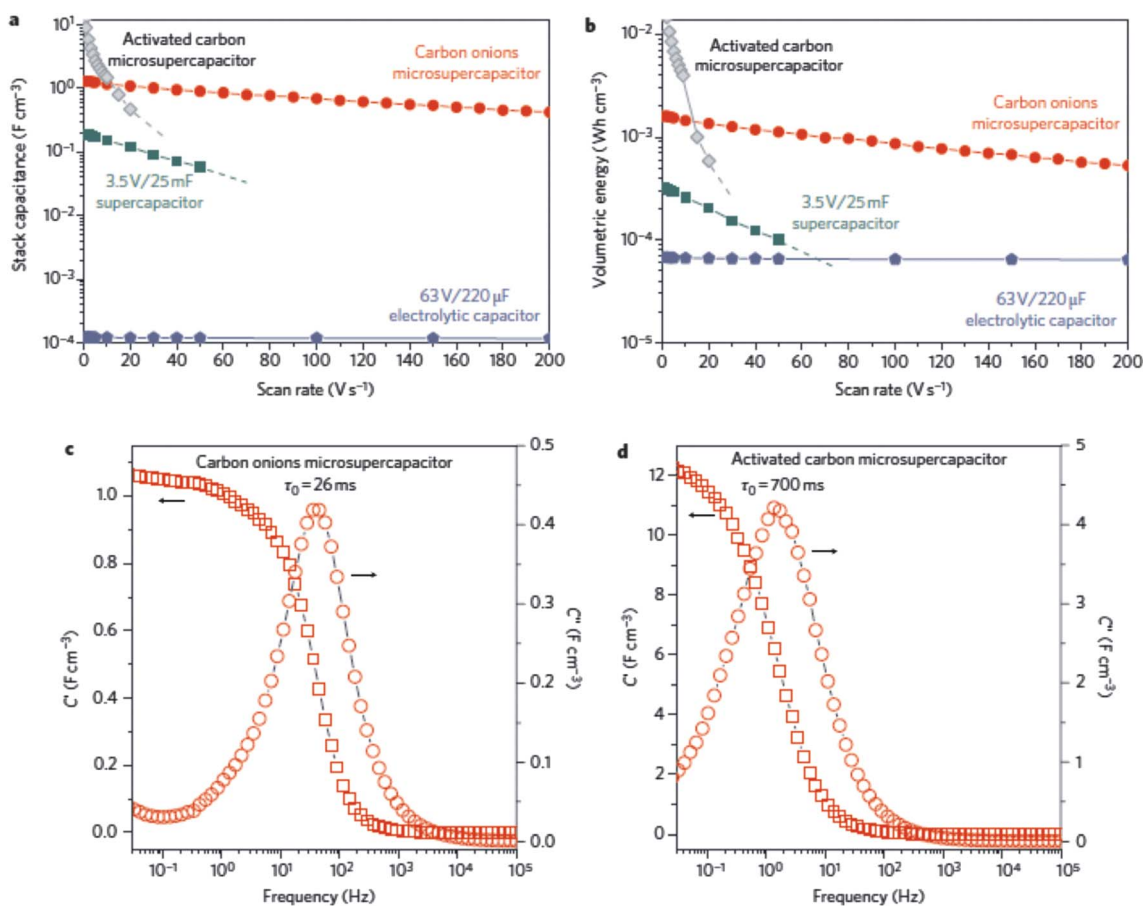

Fig. 6 Comparison of microsupercapacitors and other energy storage devices: (a) evolution of the stack capacitance *versus* scan rates; (b) evolution of the volumetric energy of the different energy-storage devices; (c) and (d) evolution of the real and imaginary part (C' and C'') of the stack capacitance of microdevices based on (c) CNOs and (d) AC (reproduced with permission from MPL).[57]

of CNO surfaces to ion adsorption/desorption, these devices show extremely small characteristic relaxation time constants ($\tau \sim 26$ ms). For AC-based microdevices, the time needed to discharge all the energy from the device with an efficiency of 50% is 700 ms.

Carbon nano-onions produced at high temperatures (1800 °C) showed the best performance in terms of conductivity and response rate.[55,56] The highly graphitized CNOs exhibit a constant $\tau \sim 10$ s at high charge–discharge rates of up to 50 V s^{-1}, which cannot be matched by any other carbon form.

To the best of our knowledge, there are no other reported devices that show similar performance characteristics.[58]

Cycling stability. Charging and discharging of EDLCs occur in seconds, enabling more than 1 000 000 charge and discharge cycles in relatively short times.[59] Due to the negligible chemical charge transfer reactions and phase changes occurring during the charging and discharging processes, CNO-based materials have almost unlimited cyclabilities.

Nevertheless, the cycling performance depends on the preparation conditions of the CNOs. For instance, CNOs obtained *via* stainless steel autoclave reactions from CaC_2 and $CuCl_2$ showed excellent cycling performance as anode materials for lithium-ion batteries, which can deliver a reversible capacity of 391 mA h g^{-1} for up to 60 cycles.[18] After activation in 6 M KOH CNOs showed good lifetimes.[60] After 4000 complete charge–discharge cycles, approximately 89% of the initial capacitance was preserved.

4.2. Applications

The main interest in carbon nano-onions arises from their unusual physico-chemical properties as well as from promising applications in electronics,[61,62] optics,[63] as hyperlubricants,[64] and in energy conversion and storage.[31,34,36,38,40,55–57,66–69,71,73]

Since the ability of CNOs to act as an electrically conductive medium is crucial for its numerous applications, Sek *et al.* analysed the electronic conductance of single CNO structures functionalized with sulfide terminated chains in order to trap molecules in metal–molecule–metal junctions.[61] The STM-based molecular junctions showed that electron conduction through the junctions occurs by a super exchange mechanism, and the conductances of CNOs and C_{60} are about the same order of magnitude, $\sim$71.8 μS, close to metallic behavior. This result was somewhat surprising but very promising in terms of potential applications of CNOs in molecular electronics.

Carbon nano-onions were also used as point electron sources and exhibited significant field-emission (FE) currents at 70 V.[63] CNO emitters were able to sustain a FE current of more than 100 μA, compared to only 1 μA for CNTs, mainly due to the effect of Joule heating. These new emitters showed excellent long-term stability that might serve as point electron sources for a variety of future applications.

Non-modified CNOs have somewhat limited charge accumulation properties. Thus research has focused on their chemical derivatives, which possess different physico-chemical characteristics. Chemical reactions have been used to attach different groups on their surface or to intercalate metals,[65] leading to improved solubilities and changes in their physico-chemical properties. Reactions reported include oxidation of defects,[66] fluorination,[67] radical additions,[68] 1,3-dipolar cyclo-additions,[69] and polymerization.[70] Only a few of these were aimed at obtaining CNO-based materials for supercapacitor electrodes.

Although the study of CNOs in EDLCs is not extensively documented, recent studies revealed that they are competitive relative to other carbon nanostructures. Due to their advantageous properties, CNO materials are being used in a variety of

Table 4 Specific capacitance values of CNOs for supercapacitors

Types of materials	Specific capacitance (F g^{-1})	Reference
CNO	7.18	80
CNOs/KOH activation	<122	54
CNOs/H_2SO_4 activation	20–40	66,73
ox-CNOs[a]	3.69	69
oz-CNOs[b]	<43.40	70
CNOs/RuO_2xH_2O	27–334	79
CNOs/4-ABAC	<34.44	72
CNOs/PDDA	9.26–33.41	80
CNOs/chit	8.53–32.07	80
CNOs/PANI	110–506	72,81
CNOs/PEDOT:PSS	35.16–96.47	82
ox-CNOs/PEDOT:PSS	<49.05	82
ox-CNOs/C_{60}–Pd	<280	83

4-ABAC – 4-aminobenzoic acid; chit – chitosan; oz-CNOs – the ozone treatment of CNOs; ox-CNOs – CNOs oxidized in 3 M HNO_3; PANI – polyaniline; PEDOT:PSS – poly(3,4-ethylenedioxythiophene):poly(styrenesulfonate); PDDA – poly(diallyldimethylammonium chloride).

[a] for 0.1 M $HClO_4$. [b] for 0.1 M Na_2SO_4.

carbon electrodes. Wettability is one of these properties, which is mainly determined by the surface functionalities and affects the capacitance of organic or aqueous supercapacitors. Chemical modification of CNO surfaces has been achieved through a variety of methods: chemical treatment with nitric and/or
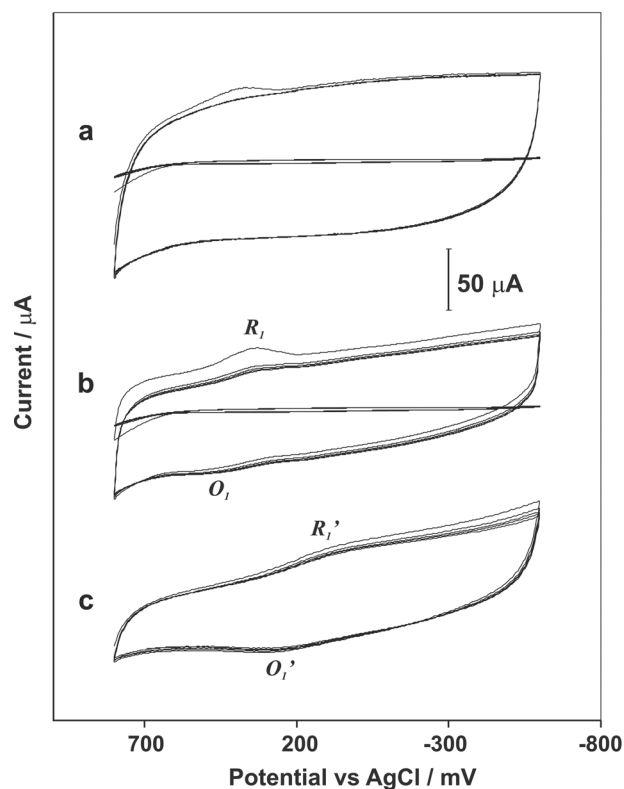

Fig. 7 Cyclic voltammograms of (a) CNO/TOABr, (b) ox-CNO/TOABr, and (c) ox-CNO films in 0.1 M NaCl (ox-CNOs: oxidized CNOs, TOABr: tetra(*n*-octyl) ammonium bromide). The sweep rate was 100 mV s^{-1} (reproduced with permission from ECS).[71]

sulfuric acids,[71] chemical activation with potassium hydroxide,[54] ozone treatment,[72] and covalent functionalization with acid derivatives.[73] Promising capacitance values (see Table 4), ranging between 20 and 40 F g^{-1} and 70–100 F g^{-1} were found in acid electrolytic solution (1 M H_2SO_4) and alkaline solution (6 M KOH), respectively.[54,66,74]

When carbon materials are oxidized with extremely aggressive agents, their hydrophilicity increases because of an increase in the concentration of oxygen atoms on the carbon nanostructures.[75] On the other hand, this process causes damage and structural changes on the carbon surfaces by disrupting the conjugated graphitic structure and the resistivity is simultaneously increased.[7,8] For these materials, the voltammetric characteristics change from the typical rectangular shape to the one exhibiting a faradaic component at *ca.* 0.2 V (see Fig. 7b and c). The broad and poorly defined peaks were recorded for voltammograms in cathodic and anodic cycles and were related to the reduction of the –COOH group to –CH_2OH.[76]

Mild ozone treatment leads to larger total surface areas and higher micropore volumes.[77] This modification provides a method to produce lactone, hydroxyl and phenolic functional groups on the surface of CNOs.[72] This process does not cause severe damage or structural changes to the carbon surfaces by disrupting their graphitic structure. For electrodes prepared under the same conditions, ozonolysis provides both increased hydrophilicity and conductivity for improved performance of aqueous type EDLCs, which exhibit about 20 times larger specific capacitances (43.40 F g^{-1}) than those oxidized in 3 M HNO_3 CNOs (2.29 F g^{-1}).[69,71,72]

Since the limited accessibility of non-modified carbon surfaces to the electrolyte in CNO EDLCs affects the performance of a supercapacitor, an effective approach is to modify the CNOs with pseudocapacitive redox materials, including transition metal oxides,[79] and conducting polymers,[72,81,82] to form composites.[78] This approach combines the large pseudocapacitance from the redox-capacitive materials with the robustness of CNOs and produces composites with superior electrochemical properties.

Composites including carbon nano-onions for supercapacitor electrodes can be considerably improved for charge storage, but the number of published articles concerning CNO functionalization for this purpose is still very sparse. Only a few articles have reported the synthesis and the electrochemical characteristics of CNOs. Enhancement of the specific capacitance for CNO-based materials was accomplished by the following modifications:

(1) the formation of CNO/conducting polymer composites;[72,81,82]

(2) the formation of CNO/solid polyelectrolyte composite;[80]

(3) insertion of electroactive particles of transition metals or metal oxides.[79,83]

Specific capacitance values of different CNO-based materials for supercapacitor applications are summarized in Table 4. Composite materials based on the integration of carbon structures with other substances can lead to materials possessing properties of the individual components. During the modification of carbon materials many parameters, such as the degree of hydration and

crystallinity of transition metal oxides, the potential degradation of conducting polymers, and the decrease of the surface area of the composites, have to be taken into consideration for the preparation of optimal composite electrodes for supercapacitors.

5. Conclusions and future outlook

Carbon nano-onions are excellent supercapacitor electrode materials for high rate and high power applications, especially for microsupercapacitors. Because of their structure and high degree of graphitization, CNOs are able to maintain 80% of their capacitance at scan rates of 15 V s^{-1}. There are three main routes by which the capacitive energy storage can be improved:[84]

(1) by preparing highly porous structures with much larger areas per square centimetre;

(2) by increasing the polarizabilities at the electrochemical interface;

(3) by using nonaqueous systems, particularly pure liquid electrolytes at room temperature.

Although CNO-based EDLCs exhibit many advantages, many challenges still remain. Since it has been shown theoretically that the positive curvature causes the normalized capacitance to increase with decreasing particle size, optimizing a synthetic method to obtain the smallest possible CNO particles is important. The continued development of synthetic, processing and material fabrication protocols that enable highly pure, reproducible CNO structures is required, if their true potential is to be realised. New synthetic and purification methods need to be designed. The use of CNOs requires improvement of the quality and homogeneity of the samples and the availability of reliable methods for their preparation, to control the number of graphitic layers. Considerable progress has been made along these lines and separations are improving.

Although CNO electrodes can deliver/recover very quickly, their energy density is a limitation for commercial devices. The density of the electrode material will affect significantly the capacitor performance and parameters such as the gravimetric and volumetric energy of the device. Very porous surface areas of carbon electrode materials result in low densities. For instance, commercial batteries possess capacitances >50 W h kg^{-1}, while commercially available carbon-based materials exhibit capacitances of only 3–4 W h kg^{-1}. The most important challenge for improved CNO-EDLCs is to increase the device energy density, making them comparable to batteries. With this aim, two main research directions should be developed.

(i) Design carbon forms with optimized and homogenous distribution of pore structures to increase their specific surface capacitances. Understanding the effect of surface chemistry, carbon conductivity and ion confinement in nanopores on the capacitance is still lacking. Thus, it is important to design the carbon–electrolyte interface to optimize the adsorption of ions from the electrolyte in order to maximize the charge stored per unit of weight or volume of carbon.

(ii) Design hybrid systems where one supercapacitor electrode is associated with faradaic processes in an organic or aqueous electrolyte.

Many challenges remain, particularly with regard to characterizing and understanding the physical, chemical, and electrochemical interactions within multicomponent systems including CNOs.

Acknowledgements

Notes and references

1 D. R. Rolison, J. W. Long, J. C. Lytle, A. E. Fischer, C. P. Rhodes, T. M. McEvoy, M. E. Bourga and A. M. Lubers, *Chem. Soc. Rev.*, 2009, **38**, 226; G. G. Wallace, J. Chen, D. Li, S. E. Moulton and J. M. Razal, *J. Mater. Chem.*, 2010, **20**, 3553; S. A. Sherrill, P. Banerjee, G. W. Rubloff and S. B. Lee, *Phys. Chem. Chem. Phys.*, 2011, **13**, 20714; A. Walcarius, *Chem. Soc. Rev.*, 2013, **42**, 3649; L. Duclaux, E. Frackowiak and F. Beguin, *J. Power Sources*, 1999, **81–82**, 323.

2 D. R. Rolison, J. W. Long, J. C. Lytle, A. E. Fischer, C. P. Rhodes, T. M. McEvoy, M. E. Bourg and A. M. Lubers, *Chem. Soc. Rev.*, 2009, **38**, 226.

3 J. Chmiola, G. Yushin, Y. Gogotsi, C. Portet, P. Simon and P. L. Taberna, *Science*, 2006, **313**, 1760; A. G. Pandolfo and A. F. Hollenkamp, *J. Power Sources*, 2006, **157**, 11; M. D. Levi, G. Salitra, N. Levy and D. Aurbach, *Nat. Mater.*, 2009, **8**, 872.

4 B. E. Conway, *Electrochemical Supercapacitors: Scientific Fundamentals and Technological Applications*, Kluwer Academic/Plenum Publisher, New York, 1999.

5 R. Kötz and M. Carlen, *Electrochim. Acta*, 2000, **45**, 2483.

6 R. Kötz and M. Carlen, *Electrochim. Acta*, 2000, **45**, 2483.

7 G. Wang, L. Zhang and J. Zhang, *Chem. Soc. Rev.*, 2012, **41**, 797.

8 E. Frackowiak and F. Beguin, *Carbon*, 2001, **39**, 937; E. Frackowiak, *Phys. Chem. Chem. Phys.*, 2007, **9**, 1774.

9 F. Beguin and E. Frackowiak, Carbons for Electrochemical Energy Storage and Systems in *Advances Materials and Technologies Series*, ed. Y. Gogotsi, CRC Press, Taylor & Francis Group, 2010.

10 S. Bose, T. Kuila, A. K. Mishra, R. Rajasekar, N. H. Kim and J. H. Lee, *J. Mater. Chem.*, 2012, **22**, 767.

11 P. Simon and Y. Gogotsi, *Acc. Chem. Res.*, 2013, **46**, 1094.

12 D. Ugarte, *Nature*, 1992, **359**, 707.

13 V. L. Kuznetsov, A. L. Chuvilin, Y. V. Butenko, I. Y. Malkov and V. M. Titov, *Chem. Phys. Lett.*, 1994, **222**, 343; J. Qian, C. Pantea, J. Huang, T. W. Zerda and Y. Zhao, *Carbon*, 2004, **42**, 2691; S. Tomita, M. Fujii, S. Hayashi and K. Yamamoto, *Diamond Relat. Mater.*, 2000, **9**, 856; Q. Zou, Y. G. Li, B. Lv, M. Z. Wang, L. H. Zou and Y. C. Zhao, *Inorg. Chem.*, 2010, **46**, 127.

14 N. Sano, H. Wang, M. Chhowalla, I. Alexandrou and G. A. J. Armatunga, *Nature*, 2001, **414**, 506; N. Sano,

H. Wang, I. Alexandrou, M. Chhowalla, K. B. K. Teo and G. A. J. Armatunga, *J. Appl. Phys.*, 2002, **92**, 2783; I. Alexandrou, H. Wang, N. Sano and G. A. J. Armatunga, *J. Chem. Phys.*, 2004, **120**, 1055.

15 M. Choucair and J. A. Stride, *Carbon*, 2012, **50**, 1109.

16 T. Cabioc'h, M. Jaouen, E. Thune, P. Guerin, C. Fayoux and M. F. Denanot, *Surf. Coat. Technol.*, 2000, **128**, 43.

17 X. H. Chen, F. M. Deng, J. X. Wang, H. S. Yang, G. T. Wu, X. B. Zhang, J. C. Peng and W. Z. Li, *Chem. Phys. Lett.*, 2001, **336**, 201; A. G. Nasibulin, A. Moisala, D. P. Brown and E. I. Kaupinnen, *Carbon*, 2003, **41**, 2711; Y. Z. Yang, X. G. Liu and B. S. Xu, *J. Mater. Res.*, 2008, **23**, 1393; C. G. Zhang, J. J. Li, C. S. Shi, E. Z. Liu, X. W. Du and N. Q. Zhao, *Carbon*, 2011, **49**, 1151.

18 F.-D. Han, B. Yao and Y.-J. Bai, *J. Phys. Chem. C*, 2011, **115**, 8923.

19 M. Choi, I. S. Altman, Y.-J. Kim, P. V. Pikhitsa, S. Lee, G.-S. Park, T. Jeong and J.-B. Yoo, *Adv. Mater.*, 2004, **16**, 1721; T. Gorelik, S. Urban, F. Falk, U. Kaiser and U. Glatzel, *Chem. Phys. Lett.*, 2003, **373**, 642; L. Hu, S. Wang, B. Zhang and Y. Zeng, *Carbon*, 2006, **44**, 1725; Y. Gao, Y. S. Zhou, J. B. Park, H. Wang, X. N. He and H. F. Luo, *Nanotechnology*, 2011, **22**, 165604.

20 Z. Qiao, J. Li, N. Zhao, C. Shi and P. Nash, *Chem. Phys. Lett.*, 2006, **429**, 479.

21 S. Tomita, T. Sakurai, H. Ohta, M. Fujii and S. Hayashi, *J. Chem. Phys.*, 2001, **114**, 7477.

22 R. Bacon, *J. Appl. Phys.*, 1960, **31**, 284.

23 F. Benhart and P. M. Ajayan, *Nature*, 1996, **382**, 433; Y. Gan and F. Banhart, *Adv. Mater.*, 2008, **20**, 4751; I. V. Ponomareva and L. A. Chernozatonskii, *Microelectron. Eng.*, 2003, **69**, 625; S. Tomita, M. Fujii, S. Hayashi and K. Yamamoto, *Diamond Relat. Mater.*, 2000, **9**, 856; P. Redlich, F. Banhart, Y. Lyutovich and P. M. Ajayan, *Carbon*, 1998, **5–6**, 561.

24 J. Y. Huang, *Nano Lett.*, 2007, **7**, 2335; F. Banhart, T. Fuller, P. Redlich and P. M. Ajayan, *Chem. Phys. Lett.*, 1997, **269**, 349; Y. Gan and F. Banhart, *Adv. Mater.*, 2008, **20**, 4751.

25 L. Wei, M. Sevilla, A. B. Fuertes, R. Mokaya and G. Yushin, *Adv. Energy Mater.*, 2011, **1**, 356.

26 L. L. Zhang, R. Zhou and X. S. Zhao, *J. Mater. Chem.*, 2010, **20**, 5983.

27 V. Presser, M. Heon and Y. Gogotsi, *Adv. Funct. Mater.*, 2011, **21**, 810.

28 A. G. Pandolfo and A. F. Hollenkamp, *J. Power Sources*, 2006, **157**, 11.

29 L. Permann, M. Latt, J. Leis and M. Arulepp, *Electrochim. Acta*, 2006, **51**, 1274.

30 A. Palkar, F. Melin, C. M. Cardona, B. Elliott, A. K. Naskar, D. D. Edie, A. Kumbhar and L. Echegoyen, *Chem.–Asian J.*, 2007, **2**, 625.

31 T. Pichler, M. Knupfer, M. S. Golden, J. Fink and T. Cabioc'h, *Phys. Rev. B: Condens. Matter Mater. Phys.*, 2001, **63**, 155415.

32 C. Portret, G. Yushin and Y. Gogotsi, *Carbon*, 2007, **45**, 2511.

33 J. K. McDonough, A. I. Frolov, V. Presser, J. Niu, C. H. Miller, T. Ubieto, M. V. Federov and Y. Gogotsi, *Carbon*, 2012, **50**, 3298.

34 G. Feng, D. Jiang and P. T. Cummings, *J. Chem. Theory Comput.*, 2012, 1058.

35 C. Portret, J. Chmiola, Y. Gogotsi, S. Park and K. Lian, *Electrochim. Acta*, 2008, **53**, 7675.

36 S. Brunauer, P. H. Emmett and E. Teller, *J. Am. Chem. Soc.*, 1938, **60**, 309.

37 J. Chmiola and Y. Gogotsi, *Nanotechnol. Law Bus.*, 2007, **4**, 577.

38 W. Li, G. Reichenauer and J. Fricke, *Carbon*, 2002, **40**, 2955.

39 G. Salitra, A. Soffer, L. Eliad, Y. Cohen and D. Aurback, *J. Electrochem. Soc.*, 2000, **147**, 2486; C. Vix-Guterl, E. Frackowiak, K. Jurewicz, M. Friebe, J. Parmantier and F. Beguin, *Carbon*, 2005, **43**, 1293; L. Eliad, G. Salitra, A. Soffer and D. Aurbach, *Langmuir*, 2005, **21**, 3198; R. Lin, P. Huang, J. Segalini, C. Largeot, P. L. Taberna, J. Chmiola, Y. Gogotsi and P. Simon, *Electrochim. Acta*, 2009, **54**, 7025.

40 A. G. Pandolfo, G. J. Wilson, T. D. Huynh and A. F. Hollenkamp, *Fuel Cells*, 2010, **5**, 856.

41 E. Raymundo-Pinero, K. Kierczek, J. Machnikowski and F. Begiun, *Carbon*, 2006, **44**, 2498; J. Chmiola, G. Yushin, Y. Gogotsi, C. Portret, P. Simon and P. L. Taberna, *Science*, 2006, **313**, 1760; J. Chmiola, C. Largeot, P.-L. Taberna, P. Simon and Y. Gogotsi, *Angew. Chem., Int. Ed.*, 2008, **47**, 3392.

42 C. Largeot, C. Portret, J. Chmiola, P.-L. Taberna, Y. Gogotsi and P. Simon, *J. Am. Chem. Soc.*, 2008, **130**, 2730.

43 M. Inagaki, *New Carbons Control of Structure and Functions*, Elsevier, Amsterdam, 2000.

44 R. C. Bansal, J. Donnet and F. Stoeckli, *Active Carbon*, Marcel Dekker, New York, 1988.

45 S. Kondrat, C. R. Perez, V. Presser, Y. Gogotsi and A. A. Kornyshev, *Energy Environ. Sci.*, 2012, **5**, 6474.

46 T. A. Centeno, O. Seredab and F. Stoeckli, *Phys. Chem. Chem. Phys.*, 2011, **13**, 12403.

47 R. De Levie, *Electrochim. Acta*, 1963, **8**, 751; R. De Levie, *Electrochim. Acta*, 1964, **9**, 1231; H. Keiser, K. D. Beccu and M. A. Gutjhar, *Electrochim. Acta*, 1976, **21**, 539; H. K. Song, Y. H. Yung, K. H. Lee and L. H. Dao, *Electrochim. Acta*, 1999, **44**, 3513.

48 P. L. Taberna, P. Simon and J. F. Fauvarque, *J. Electrochem. Soc.*, 2003, **148**, A292; P. L. Taberna, C. Portret and P. Simon, *Appl. Phys. A*, 2006, **82**, 639.

49 I. Tanahashi, A. Yoshida and A. Nishino, *Bull. Chem. Soc. Jpn.*, 1990, **63**, 3611.

50 J. S. Huang, B. G. Sumpter, V. Meunier, G. Yushin, C. Portret and Y. Gogotsi, *J. Mater. Res.*, 2010, **25**, 1525.

51 Y. Sun, Q. Wu and G. Shi, *Energy Environ. Sci.*, 2011, **4**, 1113.

52 S. Li, G. Feng, P. F. Fulvio, P. C. Hillesheim, C. Liao, S. Dai and P. T. Cummings, *J. Phys. Chem. Lett.*, 2012, **3**, 2465.

53 R. Lin, P.-L. Taberna, S. Fantini, V. Presser, C. R. Perez, F. Malbosc, N. L. Rupeinghe, K. B. K. Teo, Y. Gogotsi and P. Simon, *J. Phys. Chem. Lett.*, 2011, **2**, 2396.

54 R. Costa, C. M. Pereira and F. Silva, *Phys. Chem. Chem. Phys.*, 2010, **12**, 11125; V. Lockett, R. Sedev, J. Ralston, M. Horne and T. Rodopolous, *J. Phys. Chem. C*, 2008, **112**, 7486; F. Silva, C. Gornes, M. Figueiredo, R. Costa, A. Martins and C. M. Pereira, *J. Electroanal. Chem.*, 2008, **622**, 153.

55 E. A. Ukshe, N. G. Bukun, D. I. Leikies and A. N. Frumkin, *Electrochim. Acta*, 1964, **9**, 431.

56 P. Simon and Y. Gogotsi, *Philos. Trans. R. Soc., A*, 2010, **368**, 3457.

57 D. Pech, M. Brunet, H. Durou, P. Huang, V. Mochalin, Y. Gogotsi, P.-L. Taberna and P. Simon, *Nat. Nanotechnol.*, 2010, **5**, 651.

58 P. Banerjee, I. Perez, L. Henn-Lecordier, S. B. Lee and G. W. Rubloff, *Nat. Nanotechnol.*, 2009, **4**, 292.

59 P. Simon and A. Burke, *Electrochem. Soc. Interface*, 2010, **17**, 38.

60 Y. Gao, Y. S. Zhou, M. Qian, X. N. He, J. Redepenning, P. Goodman, H. M. Li, L. Jiang and Y. F. Lu, *Carbon*, 2013, **51**, 52.

61 S. Sek, J. Breczko, M. E. Plonska-Brzezinska and L. Echegoyen, *ChemPhysChem*, 2013, **14**, 96.

62 M.-S. Wang, D. Goldberg and Y. Bondo, *ACS Nano*, 2010, **4**, 4396.

63 S. Tomita, M. Fujii and S. Hayashi, *Phys. Rev. B: Condens. Matter Mater. Phys.*, 2002, **66**, 245424; V. L. Kuznetzov, S. I. Moseenkov, K. V. Elumeeva, T. V. Larina, V. F. Anufrienko, A. I. Romanenko, O. B. Anikeeva and E. N. Tkachev, *Phys. Status Solidi B*, 2011, **248**, 2572; T. Cabioc'h, S. Camelio, L. Henrard and P. Lambin, *Eur. Phys. J. B*, 2000, **18**, 535.

64 Y. Liu, R. L. Vander Wal and V. N. Khabashesku, *Chem. Mater.*, 2007, **19**, 778.

65 Y. V. Butenko, A. K. Chakraborty, N. Peltekis, S. Krishnamurthy, V. R. Dhanak, M. R. C. Hunt and L. Siller, *Carbon*, 2008, **46**, 1133; D. Santiago, G. G. Rodriguez-Calero, A. Palkar, D. Barraza-Jimenez, D. H. Galvan, G. Casillas, A. Mayoral, M. Jose-Yacaman, L. Echegoyen and C. R. Cabrera, *Langmuir*, 2012, **28**, 17202; T. Oku, G. Schmid and K. Suganuma, *J. Mater. Chem.*, 1998, **8**, 2113; C. N. He, N. Q. Zhao, C. S. Shi, X. W. Du and J. J. Li, *J. Alloys Compd.*, 2009, **472**, 230.

66 J. Luszczyn, M. E. Plonska-Brzezinska, A. Palkar, A. T. Dubis, A. Simionescu, D. T. Simionescu, B. Kalska-Szostko, K. Winkler and L. Echegoyen, *Chem.–Eur. J.*, 2010, **16**, 4870.

67 Y. Liu, R. L. Vander Wal and V. N. Khabashesku, *Chem. Mater.*, 2007, **19**, 778.

68 L. Zhou, C. Gao, D. Zhu, W. Xu, F. F. Chen, A. Palkar, L. Echegoyen and E. S.-W. Kong, *Chem.–Eur. J.*, 2009, **15**, 1389.

69 C. T. Cioffi, A. Palkar, F. Melin, A. Kumbhar, L. Echegoyen, M. Melle-Franco, F. Zerbetto, G. M. Aminur Rahman, C. Ehli, V. Sgobba, D. M. Guldi and M. Prato, *Chem.–Eur. J.*, 2009, **15**, 4419; K. Flavin, M. N. Chaur, L. Echegoyen and S. Giordani, *Org. Lett.*, 2010, **12**, 840; V. Georgakilas, D. M. Guldi, R. Signorini, R. Bozio and M. Prato, *J. Am. Chem. Soc.*, 2003, **125**, 14268.

70 A. S. Rettenbacher, B. Elliott, J. S. Hudson, A. Amirkhanian and L. Echegoyen, *Chem.–Eur. J.*, 2006, **12**, 376; S. Rettenbacher, M. W. Perpall, L. Echegoyen, J. Hudson and D. W. Smith, *Chem. Mater.*, 2007, **19**, 1411; L. Zhou, C. Gao, D. Zhu, W. Xu, F. F. Chen, A. Palkar, L. Echegoyen and E. S.-W. Kong, *Chem.–Eur. J.*, 2009, **15**, 1389;

This journal is © The Royal Society of Chemistry 2013

J. Mater. Chem. A, 2013, **1**, 13703–13714 | **13713**

O. Shenderova, C. Jones, V. Borjanovic, S. Hens, G. Cunningham, S. Mossenkov, V. Kuznetsov and G. McGuire, *Phys. Status Solidi A*, 2008, **205**, 2245.

71 M. E. Plonska-Brzezinska, A. Palkar, K. Winkler and L. Echegoyen, *Electrochem. Solid-State Lett.*, 2010, **13**(4), K35.

72 M. E. Plonska-Brzezinska, A. Lapinski, A. Z. Wilczewska, A. T. Dubis, A. Villalta-Cerdas, K. Winkler and L. Echegoyen, *Carbon*, 2011, **49**, 5079.

73 M. E. Plonska-Brzezinska, J. Mazurczyk, J. Breczko, B. Palys, A. Lapinski and L. Echegoyen, *Chem.–Eur. J.*, 2012, **18**, 2600.

74 E. G. Bushueva, P. S. Galkin, A. V. Okutrub, L. G. Bulusheva, N. N. Gavrilov, V. L. Kuznetsov and S. I. Moiseekov, *Phys. Status Solidi B*, 2008, **245**, 2296.

75 J. Zhang, H. Zou, Q. Qing, Y. Yang, Q. Li, Z. Liu, X. Guo and Z. Du, *J. Phys. Chem. B*, 2003, **107**, 3712.

76 H. Luo, Z. Shi, Z. Gu and Q. Zhuang, *Anal. Chem.*, 2001, **73**, 915.

77 H. I. Chiang, P. C. Chiang and C. P. Huang, *Chemosphere*, 2002, **3**, 267.

78 X. Huang, X. Qi, F. Boey and H. Zhang, *Chem. Soc. Rev.*, 2012, **41**, 666; C.-W. Huang, C.-T. Hsieh, P.-L. Kuo and H. Teng, *J. Mater. Chem.*, 2012, **22**, 7314; M. Wu, G. A. Snook, V. Gupta, M. Shaffer, D. J. Fray and G. Z. Chen, *J. Mater. Chem.*, 2005,

15, 2297; R. B. Moghaddam and P. G. Pickup, *Phys. Chem. Chem. Phys.*, 2010, **12**, 4733; N. A. Kumar, H. J. Choi, A. Bund, J.-B. Baek and Y. T. Jeong, *J. Mater. Chem.*, 2012, **22**, 12268.

79 R. Borgohain, J. Li, J. P. Selegue and Y.-T. Cheng, *J. Phys. Chem. C*, 2012, **116**, 15068.

80 J. Breczko, K. Winkler, M. E. Plonska-Brzezinska, A. Villalta-Cerdas and L. Echegoyen, *J. Mater. Chem.*, 2010, **20**, 7761.

81 M. E. Plonska-Brzezinska, J. Breczko, B. Palys and L. Echegoyen, *ChemPhysChem*, 2013, **14**, 116; I. Kovalenko, D. G. Bucknall and G. Yushin, *Adv. Funct. Mater.*, 2010, **20**, 3979; A. Lapinski, A. T. Dubis, M. E. Plonska-Brzezinska, J. Mazurczyk, J. Breczko and L. Echegoyen, *Phys. Status Solidi C*, 2012, **9**, 1210.

82 M. E. Plonska-Brzezinska, M. Lewandowski, M. Błaszyk, A. Molina-Ontoria, L. Luciński and L. Echegoyen, *ChemPhysChem*, 2012, **13**, 4134.

83 E. Gradzka, K. Winkler, M. Borowska, M. E. Plonska-Brzezinska and L. Echegoyen, *Electrochim. Acta*, 2013, **96**, 274.

84 J. O'. M. Bockris and A. K. N. Reddy, *Modern electrochemistry*, Plenum Press, New York and London, 1998.

13714 | *J. Mater. Chem. A*, 2013, **1**, 13703–13714

This journal is © The Royal Society of Chemistry 2013